OPTOELECTRONICS AND ADVANCED MATERIALS – RAPID COMMUNICATIONS Vol. 10, No. 7-8, July-August 2016, p. 541 - 546

Optical and structural properties of chromium telluride (Cr_2Te_3) thin film produced via chemical bath deposition

İ. A. KARIPER*
Erciyes University, Education Faculty, 38039, Kayseri, Turkey

In this paper, we explain the production of chromium telluride (Cr_2Te_3) crystalline thin film via chemical bath deposition on substrates (commercial glass). Properties of the thin film, such as transmittance, absorption, optical band gap and refraction were examined in ultra-violet Spectrum. The structural properties of orthorhombic form were observed through X-ray diffraction. Structural and optical properties of Cr_2Te_3 thin films that were deposited at different pH levels were compared. Some properties of the films have changed with the change of pH, which has been deeply investigated. It has been observed that grain size of Cr_2Te_3 thin film has reached its highest value at pH 9. The refraction indexes and extinction coefficients of Cr_2Te_3 films deposited at various pH levels were calculated as 1.45, 1.82, 1.78, 1.40 (refraction index) – 0.004, 0.010, 0.009, 0.003 (extinction coefficient), for amorphous structure with 24, 42 and 63 nm average grain sizes (at 550 nm wavelength). The band gaps (Eg) of the films were measured as 2.06, 2.57, 2.04, and 2.76 eV for the grain sizes mentioned above.

(Received July 30, 2015; accepted August 3, 2016)

Keywords: Cr_2Te_3, Chemical Bath Deposition, Thin film

1. Introduction

Chemical deposition technique was used for deposition of silver and the terms used for this technique have varied in many ways, since 1835, such as chemical solution deposition (CSD), chemical bath deposition (CBD), or chemical deposition (CD). The method that we have used was discovered in 1869 and since then many different semiconductors have been deposited using this method. PbS and PbSe produced via chemical deposition technique were used as infrared detectors and has led to a progress in the military field and commercial systems [1]. CdS thin film was first produced at 1961, until this date chemical storage technique was limited with PbS and PbSe [2].Today, most of the semiconductor thin films can be produced via chemical bath deposition. Researchers choose chemical bath deposition technique because it is inexpensive and simple. However, from time to time, this method may cause troubles for the researchers. The most typical example of it is the production metal tellurium's thin films.

So far, researchers have attempted to produce semiconductors such as PBTs [4], ZnTe [4] from CdTe [3], PbTe [4], ZnTe [4] via chemical bath deposition techniques [3] using different reagents. Most of them failed, because they had obtained amorphous structures instead of crystalline structures that they have wanted. So, they either choose to anneal the film in an inert atmosphere, or make the production using technological devices. For this reason, researchers have not preferred to produce chromium telluride semiconductor thin film via CBD up to today. In fact some researchers have used CrTe thin films that they have produced using technological devices in various fields, such as field-effect capacitors [5] and tunneling magneto-resistance in magnetic tunneling junctions [6]. However there are not many studies in the literature about the optical properties of its thin film. Since the production of CrTe thin films is very difficult via wet chemical methods, no researchers has produced CrTe thin films via chemical bath deposition and no one has examined its optical properties up to now.

Currently, we do not know much about optical properties of chromium telluride thin films produced via CBD. In particular, the best known feature of chromium telluride is its magnetic property. Its ferromagnetic metallic conductivity property worth mentioning (e.g. CrTe is a metal with T_c = 340K) [7]. It has hexagonal crystal structure similar to NiAs, having optical reflectance and 3d electron transition observed between 2-4 eV. [8].One of the recent studies conducted about these films was performed by Roy et.al., where they have produced Cr_2Te_3 thin films on Al and Si substrates and they have proved that the film has showed ferromagnetic properties around 180 K [9]. These researchers have only focused on magnetic properties of the film. Since these films, which have ferromagnetic perpendicular magnetic anisotropy, are mainly used on magnetic recorders and on the devices such as spin-transfer torque (STT), the examination of these properties of the film was more attractable for many researchers.

In this study we attempted to produce chromium telluride, (Cr_2Te_3) thin film on amorphous glass via chemical bath deposition methods. The literature review that we have performed shoved that Cr_2Te_3 thin films haven't been produced via chemical bath deposition and their optical properties haven't been studied, up to now.

However, in this study we mainly focused on the optical properties of these films in order to show them they could be effectively used on opto-electronic devices as well. We tried to show that CrTe thin films can be produced via an inexpensive and simple method, and to demonstrate the usability of their optical properties. Therefore, researchers and technology world can benefit from this study.

2. Experimental method

The most important stage of this process is the preparation and production of telluride anions. 0.01 mol solid tellurium was dissolved in the 1.4 dioxin with 0.02 mole potassium hydroxide. After 30 minutes, liquid 1.4 dioxin was separated from the gel in the baker by decantation. Sodium hydrosulfite (NaHS) was added to the gel when the gel was hot. Then, the water was slowly added until the solution in the baker has become 100 mL. The pH of this main solution was around 12. However, since the pH level of the bath was very high for the deposition, it should be reduced. Another component of the bath was prepared by putting 0.01 mol chromium chloride solution in a beaker, then adding 20 mL telluride and 20 mL manganese solutions (with equal concentration) and mixing them. Glass substrates of 76x26 mm were soaped with detergent and rinsed with distilled water, then dipped into this bath.

The pH levels of the baths were adjusted to 11, 10 and 9, by adding 4, 6 and 8 mL of 25% HCl solution. The deposition duration and temperature of the bath were set as 24 hours and 20°C. pH levels of chemical baths were measured by using a pH meter (Lenko mark 6230N).

The crystalline structure of Cr_2Te_3 was confirmed by X-ray diffraction with a CuKá$_1$ radiation source (Rikagu RadB model, ë=1.5406 Å) over the range 10^o<2è<90^o at a speed of 3^o min^{-1} with a step size of 0.02^o. Surface properties of the films were examined by using an EVO 40-LEO computer controlled digital scanning electron microscope. Chemical analysis by Energy-dispersive X-ray spectroscopy was performed with an Energy-dispersive X-ray spectrometer attached to scanning electron microscope. The optical measurements were performed by Hach Lange 500 Spectrophotometer at room temperature by placing an uncoated identical commercial glass substrate to the reference beam. The optical spectrum of thin films was recorded in the wavelength at the range of 300-1100 nm. The film thicknesses were measured by Veeco Multi Mode atomic force microscopy (Controller = Nano Scope 3D). Thicknesses were measured in a 10x10 ìm area with tapping mode.

3. Results and discussion

The chemical reactions occurred during the deposition are summarized below. When chromium ions (Cr^{+3}) were added to the solution that contains telluride (Te^{-2}), chromium telluride (Cr_2Te_3) precipitation, which is not soluble in water, was formed.

$$Te_{(k)} \xrightarrow{NaSH/KOH} Te^{-2}_{(aq)} \quad (1)$$

$$2Cr^{+3}_{(aq)} + 3Te^{-2}_{(aq)} \rightarrow Cr_2Te_{3(k)} \quad (2)$$

Equations (1) and (2) show the formation of Te^{2-} and Cr_2Te_3(In an aqueous environment with a basic solution, tellurium is dissolved in the form of telluride anions).

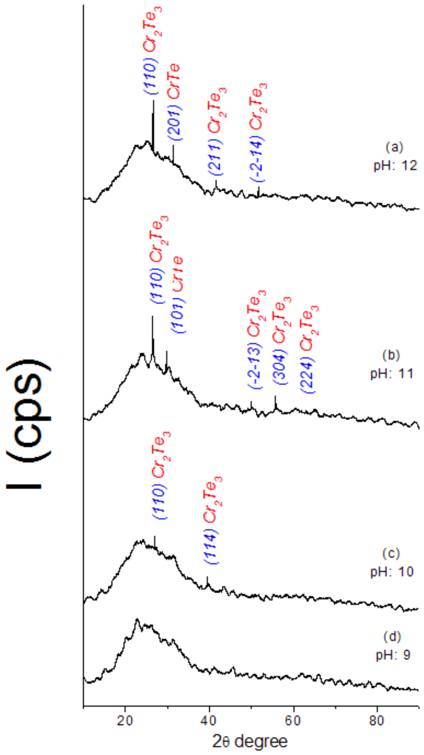

Fig. 1. X-ray patterns of Cr_2Te_3 films deposited at various pH levels: (a) pH 12, (b) pH 11, (c) pH 10 and (d) pH 9

Table 1. XRD data of ASTM values for various films

pH	ASTM Data File	ASTM Value	Observed Value	Miller İndice
12	29-458	26.142	26.605	Cr_2Te_3(110)
	71-2245	31.180	31.452	Cr_2Te_3 (201)
	71-2245	41.122	41.542	Cr_2Te_3 (211)
	71-2246	51.030	51.633	Cr_2Te_3 (-2-14)
11	29-458	26.142	26.605	Cr_2Te_3 (110)
	86-1012	29.609	29.716	CrTe (101)
	71-2246	46.579	46.768	Cr_2Te_3 (-1-23)
	26-458	55.741	55.741	Cr_2Te_3 (304)
	26-458	62.558	62.324	Cr_2Te_3 (224)
10	Unknown	Not indexing	23.356	-
	29-458	26.142	26.845	Cr_2Te_3 (110)
	29-458	39.880	39.380	Cr_2Te_3 (114)
9	Amorphous	Not indexing	Amorphous	Not indexing

Fig. 1 shows XRD patterns of various Cr_2Te_3 thin films, deposited at different pH levels (a: pH 12, b: pH 11, c: pH 10, d: pH 9). In addition to this, the comparisons of these peaks with ASTM values are presented in Table 1 (the appeared peaks). Amorphous structure was observed at pH 9, however the highest peak was observed at pH: 11. Thus, the method and the bath prepared at pH 11 can be set as the specific methodology for the production of Cr_2Te_3 thin films. A hexagonal structure was observed while indexing the structure on XRD EVA program (a= 6.829, c= 11.922 Å; Z: 4, S.G.: P-31c). The comparison of XRD results with ASTM values was in line with standard values. An unknown peak appeared at 23.356 degree. The amorphous structure obtained at pH: 9 was not indexed. In addition, a CrTe peak was detected in the film depositedat pH: 11 at 29.716 degrees. In the literature, one of the most successful studies was performed by Rot et.al. Even though they have deposited CrTe thin films on a metallic substrate (Al_2O_3) via beam epistaxy method, they have observed a single peak having (004) and (008) orientation [9]. Although the substrate on which we have deposited the films is amorphous, XRD peaks of our films are more sharp and clear (for the one deposited at pH: 12). From this point of view, the inexpensive and cheap method that we have used is more advantageous than the expensive ones, reported in the literature.

The grain size (D) of the films, which is one of the structural parameters, was analyzed from the XRD patterns and presented in Table 2. The grain size of the films was calculated from XRD patterns by using Debye Scherrer's formula,

$$D = \frac{0.9\lambda}{B cos\theta} \qquad (3)$$

where D is the grain size, ë is the wavelength of the X-ray used, â is the angular line width at half-maximum intensity in radians and è is Bragg's angle. The grain size of the films is calculated by using the following peaks of FWHM: (110) at pH 12, (110) at pH 11 and (110) at pH 10. They were, obtained through the Scherrer's method which considers the peaks of XRD patterns with maximum intensity. The unknown peak observed in the film deposited at pH: 10 and the structure of the film deposited at pH: 9 were not included in these calculations because of their amorphous structure.

The dislocation density (ä) which gives more information about the amount of defects in the films, was given by the formula,

$$\delta = \frac{1}{D^2} \qquad (4)$$

Higher δ values indicate lower crystallinity levels for the films and show the amount of defects in the structure. Larger D and smaller δ values indicate better crystallization for the films.

$$N = \frac{t}{D^3} \qquad (5)$$

where N is the number of crystallites per unit area. The higher N value indicates an abundance of crystallization.

Table 2. Grain size (D), dislocation density (δ) and number of crystallites per unit area (N) of Cr_2Te_3 thin films deposited at different pH

pH	D (nm)	$\delta\times10^{-4}$ (lines/nm^2)	$N\times10^{-3}$ (1/nm^2)	t (nm)
12	24	17.25	18.62	260
11	42	5.42	4.92	390
10	63	2.49	2.52	642

The smallest average grain size was observed for the Cr_2Te_3 films deposited at pH 12. Thin films' average grain sizes were found to be 24, 42 and 63 nm for the films deposited at pH 12, 11 and 10 respectively. The reason of lower grain size observed in the film deposited at pH 12 is the strength of the crystallization peaks. The grains stack more stringently for the materials with smaller grain size, which causes the spaces between grains to decrease. Thus, the deposition of the film on such structures leads to more orderly structures. This can be observed on XRD patterns as well. So, the peaks that we observed for the film deposited at pH 12 are in line with the results. The amorphous structure of the film deposited at pH: 9 was not evaluated, because the peaks could not be indexed.

The dislocation density (ä) of the film deposited at pH: 12 was higher than the others. The smallest average grain size was calculated for the film deposited at pH: 12 (Table 2). Even though the number of crystallites per unit area (N) of chromium telluride thin films was fix for the film deposited at pH: 12, we observed the sharpest peak at pH: 12. The film deposited at pH: 12, where maximum number of crystallites per unit area (N) was observed, was the one with the best crystalline structure, therefore this method can be set as a special method to produce chromium telluride thin film. Film thicknesses of the films were also parallel to the average grain sizes presented in Table 2.

The optic band gap energy (Eg) was calculated from the absorption spectra of the films by using the following relation:

$$(\alpha h\nu) = A(h\nu - Eg)^n \qquad (6)$$

A is a constant, α is absorption coefficient, hυ is the photon energy and n is a constant, equal to ½ for direct band gap semiconductor. The plot of $(\alpha h\upsilon)^2$ versus hυ is drawn in Fig. 2 (a: pH 12, b: pH 11, c: pH 10, d: pH 9).

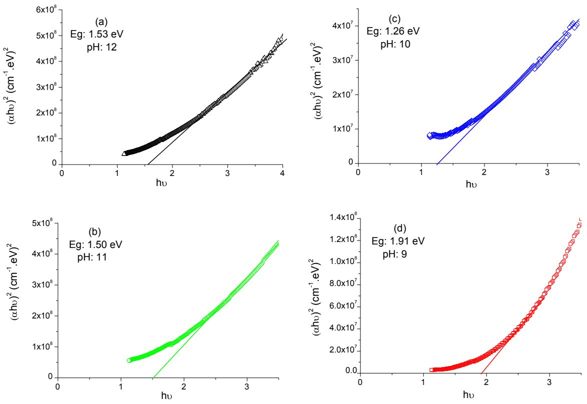

Fig. 2. Plot of (αhυ)^2 vs. hυ for Cr_2Te_3 films deposited at various pH levels: (a) pH 12, (b) pH 11, (c) pH 10, (d) pH 9

Plot of (αhυ)^2 vs. hυ for Cr_2Te_3 films deposited at different pH levels (a) pH 12, (b) pH 11, (c) pH 10, (d) pH 9 is displayed in Fig. 2. As mentioned before, we were able to control the structures of the films by controlling the pH level of the bath. This leaded to the variation of the grain sizes for each pH level and optic band gaps varied accordingly. Optic band gaps of the films were 1.53, 1.50, 1.26 and 1.91 eV for amorphous structure with 24, 42 and 63 nm average grain sizes. As can be seen, the grain size is inversely correlated with optical band gap, which was also observed by other researchers. The quantum size affects optic band gap as well [10]. To be precise, the size and electronegativity value of the atoms are the two most important factors affecting band width. This is another reason of higher optical band gap [11]. Also, the highest optical band gap was calculated for amorphous structure, where the properties of the amorphous structure were nearly equivalent to insulator materials.

The transmittance (T) of Cr_2Te_3 thin film can be calculated by using reflectivity (R) and absorbance (A) by the following expression:

$$T = (1-R)^2 e^{-A} \tag{7}$$

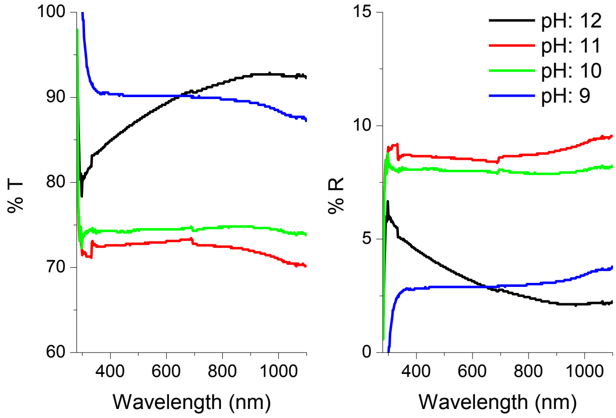

Fig. 3. Transmittance and reflectance of Cr_2Te_3 thin films deposited at various pH levels

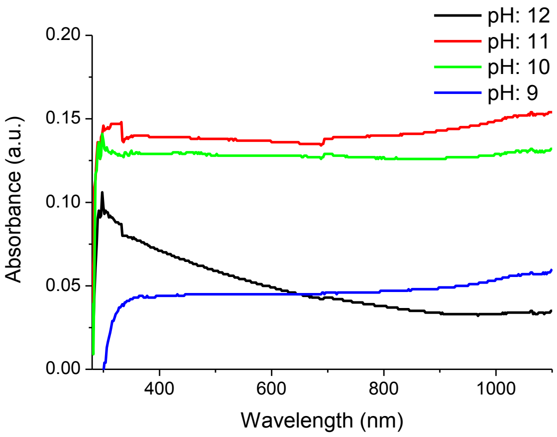

Fig. 4. Absorbance of Cr_2Te_3 thin films deposited at various pH levels

Figs. 3 and 4show the transmittance, reflectance and the absorbance of Cr_2Te_3 thin films obtained from baths with different pH levels. The lowest transmittance and the highest reflectivity values were observed for the films deposited at pH 10 and 11. This is because the absorption of the light is higher for thicker films. The absorption curve behaved as the reflectance curve and shoved an increase with the decrease of the wavelength. The transmission curve was mostly affected by the film thickness and the highest absorbance was observed for the film deposited at pH: 10 and 11. These films, especially the one produced at pH: 9, can be used as transparent thin film in the material world with its low optic band gap. Compared to the transparent thin film produced by Kawazoe et al, its transparency is higher and its optic band gap is narrower [12]. Refraction indexes and extinction coefficients of the films are calculated by the formulas:

$$n = \frac{(1+R)}{(1-R)} + \sqrt{\frac{4R}{(1-R)^2} - k^2} \tag{8}$$

$$k = \frac{\alpha\lambda}{4\pi} \tag{9}$$

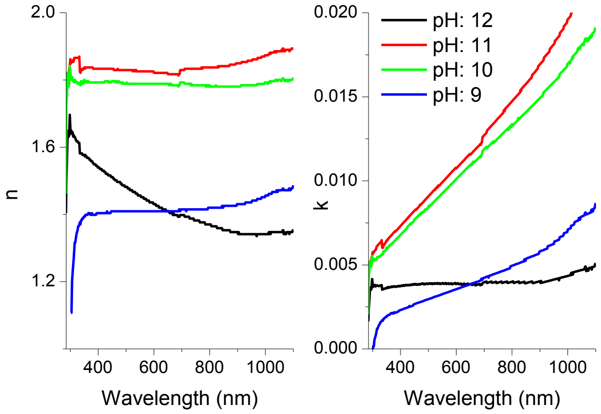

Fig. 5. Refraction index and extinction coefficient of Cr_2Te_3 films deposited at various pH levels

As can be seen from Fig. 5, refraction index and extinction coefficient of Cr_2Te_3 thin films are parallel to average grain size. Refraction indexes and extinction coefficients of Cr_2Te_3 films deposited at various pH levels were calculated as 1.45, 1.82, 1.78, 1.40 (refraction index) – 0.004, 0.010, 0.009, 0.003 (extinction coefficient) for amorphous structure with 24, 42 and 63 nm average grain sizes (at 550 nm wavelength). Refraction index and extinction coefficient have behaved in line with film thickness. The highest value of refractive index was observed as 1.82 for the film deposited at pH: 11 because of absorption. These films can be used as solid immersion lens because their refractive index is lower than 1.83 [13]. The film deposited at pH: 9 can useful for IR detectors because of its higher transmission in the visible region (% T > 90) [14]. Moreover, these films can be used for the antireflection coatings of the materials used for Fresnel reflection [15].

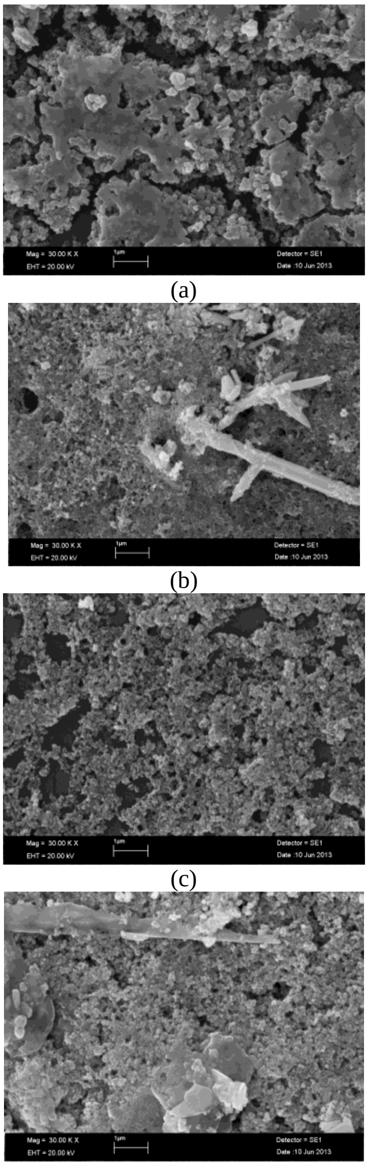

(a)

(b)

(c)

(d)

Fig. 6. SEM images of Cr_2Te_3 thin films deposited at (a) pH: 12, (b) pH: 11, (c) pH: 10, (d) pH: 9

Since surface properties directly affect the optical properties of the films, scanning electron microscopy (SEM) was used to investigate the effect of pH on the surface properties of the film. SEM images of manganese telluride thin films deposited at different pH are presented in Fig. 6. SEM analysis confirms previous outcomes. As can be seen from Fig. 6a, the best crystalline structure was observed at pH: 12, we can also observe amorphous structures as pH decreases. Although the highest grain size was calculated for the film deposited at pH: 12, some cracks can be observed on the SEM image of this film. Because of its amorphous structure, SEM image of the film deposited at pH: 9 (Fig. 6-d) has displayed a different structure than the others [16]. These results are line with XRD pattern and calculations.

4. Conclusion

In this study, a new method was developed for the production Cr_2Te_3 thin films. The production of Cr_2Te_3 thin films was tested for different pH levels, namely, 12, 11, 10 and 9. The films had the best crystallite at pH: 12; the amorphous structure was observed at pH: 9; and the grain size of the films varied as 24, 42 and 63 nm depending on the film thickness. Band gaps (Eg) of the films changed with average grain size. Refractive index and extinction coefficient of Cr_2Te_3 thin films were parallel to film thickness and grain size. Chemical bath deposition at pH: 12 can be named as a specific method for the production Cr_2Te_3.With this study, we showed that optical properties of the films, which were mostly mentioned with their magnetic properties in the literature, may also be quite useful. At the same time, we tried to enlighten the researchers about how to produce these films via an inexpensive and simple method, namely chemical bath deposition.

Acknowledgement

This study is supported by Erciyes University TeknoPark A.Ş. (ETTO).

References

[1] R. H. Bube, Photoconductivity of Solids, 1960, New York: Wiley.
[2] D. E. Bode, In: Physics of Thin Films, **3**, 275 (1966), New York and London: Academic Press.
[3] S. M. U. Ishıwu, M. N. Nnabuchı, C. N. Eze, Chalcogenide Letters **8**, 59 (2011).
[4] R. C. Alkire, D. M. Kolb, J. Lipkowski, P. N. Ross, Photoelectrochemical Materials and Energy Conversion Processes, 279 (2010P, Germany: Wiley-VCH.
[5] R. Akiyama, H. Oikawa, K. Yamawaki, S. Kuroda, Phys. Status Solidi C **11**, 1320 (2014).
[6] H. Saito, S. Yuasa, K. Ando, J. Appl. Phys. **97**, 10D305 (2005).

[7] I. Stefaniuk, M. Bester, M. Kuzma, Rev. Adv. Mater. Sci. **23**, 133 (2010).

[8] S. J. Youn, S. K. Kwon, B. I. Min, J. App. Phy. **101**, 09G522 (2007).

[9] A. Roy, S. Guchhait, R. Dey, T. Pramanik, C. C. Hsieh, A. Rai, S. K. Banerjee, ACS Nano **9**, 3772 (2015).

[10] Y. Akaltun, M. A. Yıldırım, A. Ateş, M. Yıldırım, Opt. Commun. **284**, 2307 (2011).

[11] R. Kirschman, High-Temperature Electronics, 1999, NewYork: IEEE Press.

[12] H. Kawazoe, M. Yasukawa, H. Hyodo, M. Kurita, H. Yanagi, H. Hosono, Nature **389**, 939 (1997).

[13] B. D. Terris, H. J. Mamin, D. Rugar, W. R. Studenmund, G. S. Kino, Appl. Phys. Lett. **65**, 388 (1994).

[14] E. K. Plyler, L. R. Blaine, Journal of Research of the National Bureau of Standards-C, **64**, 55 (1959).

[15] J. Q. Xi, M. F. Schubert, J. K. Kim, E. F. Schubert, M. Chen, S. Y. Lin, W. Liu, J. A. Smart, Nature Photonics **1**, 176 (2007).

[16] İ. A. Kariper, Mater & Design **106**, 170 (2016).

---

[*] Corresponding author: akariper@gmail.com